Earth and Planetary Science Letters 293 (2010) 259–268

Contents lists available at ScienceDirect

Earth and Planetary Science Letters

journal homepage: www.elsevier.com/locate/epsl

The chemical composition of the Earth: Enstatite chondrite models

M. Javoy [a], E. Kaminski [a,*], F. Guyot [a], D. Andrault [e], C. Sanloup [b], M. Moreira [a], S. Labrosse [d], A. Jambon [b], P. Agrinier [a], A. Davaille [c], C. Jaupart [a]

[a] Institut de Physique du Globe de Paris, Université Paris-Diderot, UMR CNRS 7154, 4 place jussieu, 75252 Paris cedex 05, France
[b] Université Pierre et Marie Curie, Paris, France
[c] Université Paris-Sud, Orsay, France
[d] École normale supérieure de Lyon, Lyon, France
[e] Université Blaise Pascal, Clermont-Ferrand, France

ARTICLE INFO

Article history:
Received 8 April 2009
Received in revised form 10 February 2010
Accepted 19 February 2010
Available online 27 March 2010

Editor: L. Stixrude

Keywords:
chemical earth models
enstatite chondrites
Redox state
isotopic anomalies
core composition
heterogeneous mantle
early Earth
radioactive heating

ABSTRACT

We propose a new model of Earth's bulk composition based on enstatite chondrites (E-chondrites), the only chondrite group isotopically identical to the Earth. This model allows a quantitative study of accretion and differentiation processes in the early Earth. Conditions for core formation are evaluated using data on silica–iron equilibrium at high pressure and temperature and the exchange budget equation $SiO_2 + 2Fe = Si + 2FeO$, which is the result of IW and Si–SiO_2 oxygen buffers' interaction and controls the evolution of mantle f_{O_2}. Based on that equation, ranges for the compositions of the Bulk Silicate Earth, the lower mantle and the core are deduced from the compositions of E-chondrites and their constituents. For these ranges of compositions, we show that during core differentiation, the mantle f_{O_2} evolves naturally from ≈IW-3.2 to IW-1.4 ± 0.1. The model compositions are tightened using geophysical constraints on (1) the amount of light elements in the core, (2) the petrology of the upper and lower mantle and (3) the thermal and convective structure of the lower mantle. Our results indicate that the lower mantle is enriched in Si and Fe, which is consistent with recent geophysical studies, and depleted in highly refractory elements, notably in Uranium and Thorium.

1. Introduction

The Bulk Earth composition must be specified for models of accretion and differentiation, as well as for mantle convection calculations. This composition is rarely derived from an estimate of the starting material. Instead, it is often obtained from a Primitive Upper Mantle (PUM) composition deduced from terrestrial data and chondritic constraints (e.g. Hart and Zindler, 1986; McDonough and Sun, 1995; Lyubetskaya and Korenaga, 2007). With the hypothesis that the Earth's mantle is homogeneous, the PUM composition is extended to the whole silicate Earth. Other determinations of the Bulk Earth composition (e.g. Ringwood, 1979; Allègre et al., 1995) also rely on the hypothesis of a homogeneous mantle. One difficulty with these models is that they cannot be assessed against independent data on the mantle and core of Earth, so that they can be considered as "open-ended".

The model of a homogeneous mantle (at least for major elements) has been challenged by recent geophysical studies that advocate a chemically distinct lower mantle (e.g. Stixrude et al., 1992; Anderson, 2002; Cammarano and Romanowicz, 2007). Different interpretations of the geophysical data stem from various trade-offs between the thermal structure, the iron concentration and the silicate perovskite content of the lower mantle (Deschamps and Trampert, 2004). For example, Verhoeven et al. (2009), using electromagnetic and seismic data, suggest that the lower mantle is characterized by a progressive decrease of its perovskite content and a constant iron content, whereas Khan et al. (2008), using geodetic and seismic data, propose a lower mantle that is enriched in iron and depleted in silicium. Thus, current geophysical data cannot provide a precise estimate of lower mantle composition without additional constraints. An alternative strategy is to start from an estimate of the Bulk Earth composition and to evaluate the conditions of core–mantle differentiation. One may then compare the bulk mantle composition that is predicted with that of the upper mantle and hence assess the existence or absence of compositional differences between the lower and upper mantle.

Here, we argue in favour of a specific starting material, enstatite chondrites (referred to as E-chondrites in the following), which have the same isotopic composition as Earth. Relying on a pyrolitic composition for the Primitive Upper Mantle (PUM) and on a mechanism for core–mantle differentiation, we obtain a range of compositions for the Bulk Silicate Earth (BSE) and for the Primitive Lower Mantle (PLoM). The

* Corresponding author.
E-mail address: kaminski@ipgp.fr (E. Kaminski).

0012-821X/$ – see front matter © 2010 Elsevier B.V. All rights reserved.
doi:10.1016/j.epsl.2010.02.033

model accounts for the presence of light elements in the core as well as of oxidized iron (FeII) in the mantle. Estimates of core and mantle compositions are evaluated using geophysical data, resulting in well-defined compositions of the Bulk Earth and its major envelopes.

2. Enstatite chondrites

2.1. The isotopic parenthood of Earth and E-chondrites

All chondrite classes display significant multi-elemental isotopic differences with the Earth's mantle, with the sole exception of E-chondrites (Javoy, 1995, 2005). All elements investigated so far in E-chondrites have the same isotopic composition as terrestrial samples. This is true for oxygen (50% of the Earths atoms) (Clayton and Mayeda, 1984), nitrogen (Javoy and Pineau, 1983; Javoy et al., 1984, 1986; Javoy and Pineau, 1991; Cartigny et al., 1997), molybdenum and ruthenium (Dauphas et al., 2004), osmium (Meisel et al., 1996), radiogenic ^{53}Cr and non-radiogenic ^{54}Cr (Birck et al., 1999; Trinquier et al., 2007). Titanium is the latest addition to the list: huge ^{50}Ti and ^{46}Ti anomalies relative to the Earth's mantle are found in all meteorites save for E-chondrites (Trinquier et al., 2009). Exceptions to this rule are found for silicon and tungsten, but can be attributed to internal processes, such as core formation (e.g. Trinquier et al., 2007).

Rare gases' isotopes, commonly used as tracers of mantle dynamics, also link the Earth's mantle to E-chondrites. Mantle-derived rocks have high ^{3}He/^{4}He (7 to more than 50 times the atmospheric ratio) and ^{20}Ne/^{22}Ne ratios (higher than 12 instead of 9.8 for the atmospheric ratio—the solar wind value being 13.8.) The close-to-solar neon signature suggests that parent materials of the Earth had a solar-like signature, either a pure solar composition, or that of a solar component (Neon B) fractionated during solar wind implantation (Moreira and Allègre, 1998). The "solar" character of rare gases in E-chondrites was recognized long ago (e.g. Crabb and Anders, 1981), and appears best in their achondritic correspondents, the aubrites, such as Pesyanoe and Khortemiki (Patzer and Schultz, 2002). This solar character, found in "trapped" rare gases, is frequently "diluted" by cosmogenic noble gases, making the comparison of mantle solar and meteoritic trapped end members less accurate. The recent discovery of an enstatite chondrite particularly rich in implanted solar noble gases, SAU290, has however made this comparison very precise: its ^{20}Ne/^{22}Ne (12.96 ± 0.23), and ^{38}Ar/^{36}Ar (0.18847 ± 0.00044) ratios (Park et al., 2005) are identical to those of the Earths Lower Mantle end member (Trieloff et al., 2000; Raquin and Moreira, 2009).

2.2. The space of E-chondrite compositions

In his model of Earth composition, Javoy (1995) considered only the average EH composition, a plausible but unique composition. There is no reason, however, to suppose that the currently available E chondrite population is truly representative of the whole range of compositions. A straight average may therefore be affected by a sampling bias. The isotopic argument applies to all E-chondrites, hence it provides no criterion for discarding any specific sample. For this reason, we attempt to generate the full compositional space of E-chondrites that will, furthermore, allow tests against petrological and geophysical criteria.

E-chondrites have been separated into iron-rich EH (29 to 35% Fe) and iron-poor EL (20 to 29% Fe) (e.g. Mason, 1966; Keil, 1968; Wasson and Kallemeyn, 1988). These two meteorite families can be further subdivided according to petrological and textural characteristics, with an evolution index ranging from 3 for the most primitive objects to 6 for the most evolved (e.g. Kallemeyn and Wasson, 1986). EH are, on average, more "primitive" than EL. Finally, brecciated ("clasts") textures, like in the largest E-chondrite, Abee (Rubin, 1983) complete the description of the rich and complex history of E-chondrites (e.g. Rubin and Keil, 1983).

To reconstruct the full compositional space of E-chondrites, we take advantage of the fact that, irrespective of any classification or genetic hypothesis, all such chondrites can be described as assemblages of three groups of phases with variable chemical compositions and in variable amounts: metal, sulfide and silicate. Table 1 presents a compilation of the available mineralogical and chemical data (e.g. Keil, 1968; Rubin, 1983; Rubin and Keil, 1983; Easton, 1985; Lin and Kimura, 1998). The physical processes that have led to various proportions of the three groups in these objects are mostly the evolution from EH to EL and impact/brecciation during the accretion of planetesimals or planetary bodies, and finally differentiation leading to aubrites by differentiation (e.g. Rubin, 1983; Kong et al., 1997).

We randomly mix the three groups of phases in the variable proportions and compositions displayed in Table 1. For each element, concentration is scaled to that of the dominant element of each phase, i.e. Fe for metal, S for sulfides and Si for silicates. We use a bootstrapping technique to randomly generate these ratios using log-normal distributions with the parameters given in Table 2. The concentration of the reference element in the denominator (Fe, S or Si) is then obtained by setting the sum of elements to 100%. We consider at this stage only those elements which control the geophysically testable properties of Earth's envelopes:

- The major elements O, Si, Mg, Al, Ca, Fe, and Ni (99% of the Earth's mass) and
- The minor elements Ti, Cr, Co, Mn, and Na (most of the remaining 1%).

We have paid attention to the volatile characteristics of some of these elements. In the above list, Ca, Al and Ti are considered as refractory and totally conserved during accretion. They belong to the refractory lithophile group (thereafter RLE), whose paired ratios are considered to be constant among chondrites (e.g. Hart and Zindler, 1986). Thus, on this point we agree with classical models, and set the two ratios Ca/Al and Ca/Ti, to values in the 0.90–1.20 and 16–22 ranges, respectively (McDonough and Sun, 1995).

Some elements in the list, Mg, Si, Fe, Ni, and Cr, are considered to be transitional because of their lower condensation temperature (e.g. Wasson, 1985; Lodders, 2003) hence may be partially lost during accretion. We do not think so and we shall consider them as refractory for now, and we will justify this in the discussion of our results (Section 5.3).

Other elements in the list are volatile, namely S, Na and Mn. A large proportion of Na (and K) has clearly been lost during accretion. Their case has to be treated by correlating their terrestrial concentration to that of a RLE element (e.g. constancy of K/U and Na/Ti ratios.) The retention of Mn, with a 50% condensation temperature of 1150 ± 50 K can be tested. We have made that test in a preliminary version of the

Table 1
Phase composition (in wt.%) and proportion (in wt.%) in natural EH and EL chondrites.

Element	Silicates	Sulfides	Metal
O	48.0 ± 0.47	–	–
Si	29.7 ± 1.91	–	2.05 ± 0.92
Mg	19.5 ± 2.50	2.41 ± 2.11	–
Al	1.36 ± 0.35	0.24 ± 0.79	–
Ca	0.17 ± 0.08	4.43 ± 2.62	–
Fe	0.33 ± 0.57	52.1 ± 5.30	90.5 ± 1.36
Ni	–	0.02 ± 0.04	7.09 ± 0.90
S	–	37.4 ± 1.39	–
Ti	0.01	0.70	–
Mn	0.03	2.11	–
Cr	0.13	1.56	–
Co	–	–	0.31
Na	1.04	0.22	–
K	0.09	0.17	–
Proportion	68.3 ± 8.50	11.6 ± 4.09	20.1 ± 9.36

Table 2
Model parameters used to generate random phase assemblages in synthetic E-chondrites.

Variable	Mean	Standard deviation
$\ln(Si/Fe)_{metal}$	−3.91	0.53
$\ln(Ni/Fe)_{metal}$	−2.55	0.17
$\ln(Co/Fe)_{metal}$	−5.64	0.18
$\ln(Mg/Si)_{silicates}$	−0.38	0.20
$\ln(Al/Si)_{silicates}$	−3.11	0.35
$\ln(Ca/Si)_{silicates}$	−5.25	0.53
$\ln(Fe/Si)_{silicates}$	−3.97	0.93
$\ln(Ti/Si)_{silicates}$	−7.27	1.04
$\ln(Cr/Si)_{silicates}$	−4.91	0.27
$\ln(Mg/S)_{sulfides}$	−3.36	1.42
$\ln(Al/S)_{sulfides}$	−4.51	1.42
$\ln(Ca/S)_{sulfides}$	−2.26	0.49
$\ln(Fe/S)_{sulfides}$	0.32	0.13
$\ln(Ni/S)_{sulfides}$	−6.25	0.17
$\ln(Ti/S)_{sulfides}$	−4.13	0.59
$\ln(Cr/S)_{sulfides}$	−3.86	1.35
ln(sulfides/silicates)	−1.82	0.36
ln(metal/silicates)	−1.21	0.86

model, and the results clearly showed that Mn has been lost to a sizeable extent.

The case of sulfur is different, since it is not only volatile, but also competes with oxygen in establishing bonds with the other elements. However, sulfur is only a trace element in our planet, as shown on terrestial grounds by Dreibus and Palme (1996), Sanloup et al. (2004), and Badro et al. (2007). As detailed further in the next section, we thus consider that S has been lost in the parent material of the Earth. To account for that loss in the generated sulfide compositions, we replaced S linked to Ca, Mg, and Al by O and we removed S linked to Fe (see Reactions (2) and (3) in the next section.)

We generate 1 million sets of mixtures of phases, and give the resulting compositions in Table 3, where they are compared with the average composition of EH and EL chondrites from Wasson and Kallemeyn (1988) after desulfurization (see next section). Our average synthetic model composition of E-chondrites corresponds to a weighted average of ≈40% EH and ≈60% EL. The range of synthetic compositions is illustrated graphically in Fig. 1, where we also show natural E-chondrites compositions as well as those of aubrites and clasts. It can be seen that our composition space is consistent with all the available data. With this composition space, we are not biased by the limited sampling of E-chondrites that has been achieved so far and allow for some eccentric breccia components (clasts) and even a few of the achondritic relatives (aubrites). Applying the usual classification criteria to a random sample from our continuum of E-objects, using Al/Si, Mg/Si, Ni/Si and Fe/Si ratios normalized to CI, as in Wasson and Kallemeyn (1988), we recover the EH or EL types. These results suggest that the "true" variability of E-chondrites—as predicted by the existing variability of phase proportions and compositions—has not been fully sampled yet by the existing meteorite collections. We thus consider that the average parent material of Earth may be obtained from the synthetic population, even if its specific composition has not been found in an actual meteorite sample.

Table 3
Mean value and standard deviation for the compositions of the synthetic E-chondrites. Mean values for EH and EL from Wasson and Kallemeyn (1988) are given for comparison, with a standard deviation inferred from literature data.

Element	Mean EH (%)	Mean EL (%)	Synthetic E-chondrites (%)
O	31.1 ± 2.34	35.3 ± 2.34	33.3 ± 6.35
Si	19.0 ± 1.82	20.5 ± 1.82	20.2 ± 3.75
Mg	12.1 ± 1.85	15.5 ± 1.85	14.0 ± 3.28
Al	0.92 ± 0.30	1.16 ± 0.30	0.97 ± 0.33
Ca	0.97 ± 0.28	1.11 ± 0.28	1.00 ± 0.35
Fe	33.1 ± 4.57	24.2 ± 4.57	28.3 ± 11.9
Ni	2.00 ± 0.34	1.43 ± 0.34	1.73 ± 1.07
Ti	0.05	0.06	0.06 ± 0.02
Cr	0.36	0.34	0.36 ± 0.38
Co	0.10	0.07	0.08 ± 0.05

2.3. Critical features of E-chondrites for Earth modeling

E-chondrites' chemistry specifically display a strongly reduced character, often explained by an increase of C/O in the nebula (e.g. Kallemeyn and Wasson, 1986). Such a link between low oxygen fugacity (f_{O_2}) and high C/O in the inner nebula can be interpreted as a decrease in water fugacity (f_{H_2O}) due to water condensation beyond a few AU and/or vaporization of condensed carbon (e.g. Lodders and Fegley, 1993; Lodders, 2003). We think that these features, as well as the high temperatures recorded by E-chondrites, their large volatile contents, and their concentrations of RLE in sulfides (e.g. Petyaev and Khodakovsky, 1986; Fogel et al., 1989) can be accounted for by the action of the T-Tauri wind, which is probably also responsible for the homogeneity of their isotopic compositions. The T-Tauri wind heated the inner solar nebula to high temperatures and flushed the volatile elements, including water, out of the inner solar system. It probably vaporized the condensed carbon; it certainly vaporized the sulfur, out of its main component, troïlite. The peak temperature likely lagged behind that of the flux of volatile elements and sulfur, so that the inner planets' material was both hotter and volatile (notably sulfur)-depleted relative to the more peripheral E-chondrites, but similar in other respects and particularly in its isotopic composition and relative proportions of Si, Fe, Mg and RLE.

The very low oxygen fugacities of E-chondrites (IW-6 to IW-8) and the high temperatures they recorded (980 to 1400 K) (e.g. Petyaev and Khodakovsky, 1986; Fogel et al., 1989), in association with the very strong non ideality of Si solutions in Fe (γ_{Si} of 10^{-6} to 10^{-3}) (Schwerdtfeger and Engell, 1964; Sakao and Elliott, 1975; Fogel et al., 1989), imply a global Si enrichment of E-chondrites through the disproportionation reaction of silicon monoxide

$$2SiO = {}_{(\text{dissolved in metal})} + SiO_{2(\text{cristobalite, tridymite, quartz, glass})}. \quad (1)$$

This reduction process is strongly "silicifying" (i.e. yields high Si/Mg), a feature which classical Earth models missed completely.

The composition of E-chondrites (free silica, 2 to 4% Si in Fe) allows the calculation of [SiO+SiS] fugacities in the range of 10^{-6}–10^{-4} atm. These values may correspond to nebular pressures increased to 1–10 atm while keeping normal solar Si/H ratios. On the contrary, the sulfur pressure cannot be reconciled with a normal solar abundance at any reasonable pressure and may be the result of the volatile concentration peak flushed by the T-Tauri wind.

The high concentration of volatile elements due to the T-Tauri wind flash, and particularly the high proportion of sulfides, is likely to vanish under an increase of temperature. Such an evolution is already recorded in the EH (1000 K) to EL (1200 K) to aubrite (>1300 K) suite, where the S/Ca ratio drops from 6.8 to 3.3 and to 0.6, and the Na/Ca ratio from 0.8 to 0.55 and to 0.2 (Easton, 1985; Wasson and Kallemeyn, 1988). This decrease should be even more pronounced in the hotter Earth's formation zone and during Earth accretion. Petyaev and Khodakovsky (1986) have shown that, under the conditions of formation of E-chondrites, silicates, oxides and metals undergo reversible (de)sulfurizations such as

$$MgCaSi_2O_6 + 0.5S_2 = SiO_2 + MgSiO_3 + CaS + 0.5O_2, \quad (2)$$

$$Fe + 0.5S_2 = FeS. \quad (3)$$

The sulfurization reaction (to the right) proceeds under f_{S_2} 10 to 20 orders of magnitude greater than the coexisting f_{O_2}. This is necessary to stabilize sulfides against the intrinsically much more stable oxides

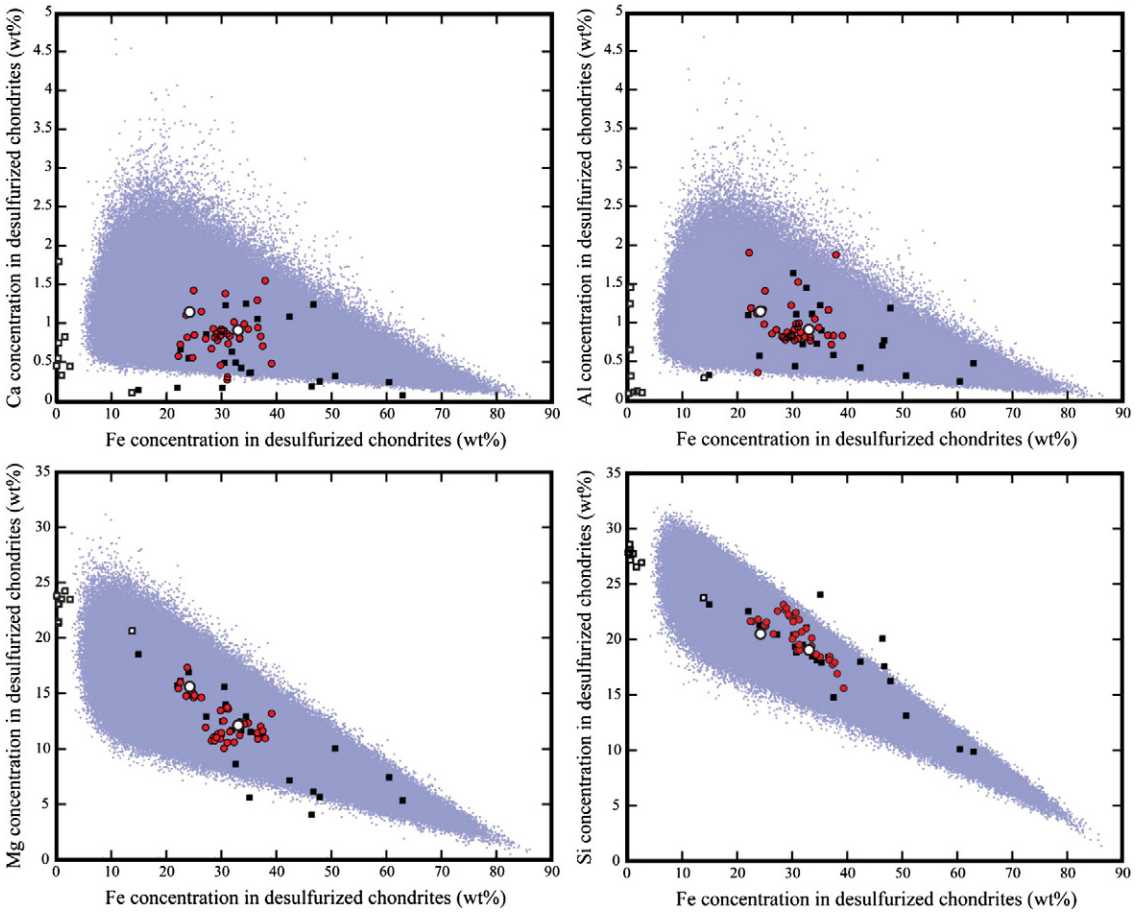

Fig. 1. Ca, Al, Mg and Si versus Fe concentration in synthetic (small dots) and natural (plain circles) E-chondrites. The big white circles stand for the average composition from Wasson and Kallemeyn (1988). The white squares are aubrites and the black squares are clasts.

and silicates. Such a f_{S_2} also points out to the abnormal and transitory character of the high f_{S_2} pulse. Desulfurization (to the left) will proceed because of the f_{S_2} decrease at the end of this pulse and/or of the increase in temperature, both likely evolutions during the course of the Earth's accretion and the waning stages of the T-Tauri phase.

A related question concerns the location of these reactions. Enstatite chondrites are generally supposed to be located in the inner part of the asteroid belt, grossly between 2 and 3 UA. They represent the outer edge of the reaction zone whereas the material of the terrestrial planets was "synthetized" closer to the Sun, in hotter regions. Since at least Wetherill and Stewart (1989), although conventional wisdom frequently states otherwise, numerical models of terrestrial planet formation have shown that only a small fraction of the Earth forming material originated from regions beyond 2.5 UA (15% in average, and down to 1.6% according to O'Brien et al. (2006)), fully in line with our postulate.

3. Composition of the Bulk Silicate Earth and of the core

All the compositions of Table 3 are not appropriate to Earth and additional constraints must be considered. The most stringent constraints are provided by the size of the core (32.4% of the total mass) and its light elements' concentration. A third constraint in our model comes from the chemical mechanism of core formation based on the reaction proposed by Javoy (1995),

$$2Fe_{metal} + SiO_2 = 2FeO + Si_{metal}. \quad (4)$$

which is now accepted as an important mechanism for core differentiation (e.g. Malavergne et al., 2004; Frost et al., 2008), and couples the FeO concentration in the mantle to the Si content of the core. A key feature of this exchange mechanism is to augment the mantle FeO and f_{O_2} without requiring the accretion of increasingly oxidized material.

With regards to this mechanism, one should note the specific character of E-chondrites: they contain pure silica, which insures maximum silica activity, and ≈50% enstatite, which also enforces higher SiO_2 activity than classical Earth's compositions. E-chondrites also contain $2 \pm 1\%$ initial Si_{metal} which contributes a significant fraction of the final equilibrium concentration. According to Malavergne et al. (2004) such an initial concentration is required to obtain ≈7% Si in the core. The increase of Simetal from 2 to 5–8% is accounted for by the reduction of 3–5% pure silica from the bulk initial material, which is available in most of our model compositions.

3.1. Internal Redox evolution

The f_{O_2} conditions for the exchange of oxygen between SiO_2 and FeO during Reaction (4) can be specified by splitting it into two "half reactions",

$$2FeO = 2Fe + O_2, \quad (5)$$

$$SiO_2 = Si + O_2, \quad (6)$$

with respective equilibrium constants K_{IW} and K_{Si-SiO_2}. Each one of these could act as an oxygen buffer fixing the f_{O_2}, if it were alone. Reaction (5) corresponds to IW buffer, for which

$$\log\left(f_{O_2}\right) = \log\left(K_{IW}(T,P)\right) + 2\log\left(a_{FeO} / a_{Fe}\right). \quad (7)$$

Reaction (6) corresponds to another potential buffer for which

$$\log\left(f_{O_2}\right) = \log\left(K_{SiO_2\text{–}Si}(T,P)\right) + \log\left(a_{SiO_2}/a_{Si}\right). \quad (8)$$

Javoy (1995) has shown that, in a closed system, SiO2 can oxidize Fe if temperatures are high enough, making f_{O_2} (i.e. $a_{FeO}/a_{Fe_{metal}}$) increase until Reaction (4) reaches equilibrium, such that the f_{O_2}'s corresponding to Reactions (6) and (5) become equal. The equilibrium constant of Reaction (4) is

$$K_e(P,T) = \frac{K_{IW}}{K_{Si\text{–}SiO_2}} \equiv \frac{a_{FeO}^2 a_{Si}}{a_{Fe}^2 a_{SiO_2}} = \frac{x_{FeO}^2 x_{Si}}{x_{Fe}^2 x_{SiO_2}} \frac{\gamma_{FeO}^2 \gamma_{Si}}{\gamma_{Fe}^2 \gamma_{SiO_2}} \equiv K_D(P,T) \frac{\gamma_{FeO}^2 \gamma_{Si}}{\gamma_{Fe}^2 \gamma_{SiO_2}}, \quad (9)$$

where a_X, x_X and γ_X are the activity, concentration, and activity coefficient of X, respectively, and where K_D is the "molar exchange coefficient" used in Frost et al. (2008).

K_e (P, T) can be calculated from the values of Gibbs free energy and volume changes from the literature (e.g. Robie and Hemingway, 1995), that predict an increase of K_e (hence of K_D) with both temperature and pressure. Experimental reactions between solid silicates and liquid metal confirm such an increase of K_e up to 25 GPa (e.g. Gessmann et al., 2001; Malavergne et al., 2004). This allows a sizeable Si uptake at relatively low P, T conditions (2–10 GPa, 1800–2200 K). In contrast, reactions between liquid silicate and liquid metal require higher P, T conditions to obtain a similar uptake, and seem to show rather a continuous decrease of K_D with pressure (Frost et al., 2008). That variety of situations makes the direct application of K_e calculation to temperatures larger than 3000 K and pressures larger than 25 GPa, rather difficult and inconclusive, as stated in Frost et al. (2008).

Because of these uncertainties, we used Reaction (4) solely as an exchange budget equation, and we checked the consistency of the results against experimental determinations.

3.2. Calculation of the core and mantle compositions

The stoichiometry of Reaction (4) is used to express the partition budget of Fe, O and Si between the core and the mantle: each mole of Si transferred from silicate to metal corresponds to $2(1-\alpha)$ moles FeO transferred to the mantle and α moles of atomic oxygen transferred to the core through the dissolution reaction $FeO \rightarrow Fe_{metal} + O_{metal}$ (Asahara et al., 2007). Thus:

$$SiO_{2silicate} + 2Fe_{metal} = Si_{core} + (2-\alpha)FeO_{mantle} + \alpha Fe_{core} + \alpha O_{core}. \quad (10)$$

For a given total amount of iron in the parent chondrite, the chosen amount of light elements sets the iron content of the core, and hence the amount of oxidized Fe in the mantle. The Fe content of the mantle sets the amount of Si in the core and thus the amount of O in the core by difference with the total light element concentration.

In order to compare our results with other core and mantle compositions from the literature, we considered that between 6 and 14% of light elements can be present in the core (Poirier, 1994), and that the iron content in the mantle may vary between4 and 14%. The concentrations of the other elements entering the core (Ni, Co and Cr) are calculated using the range of partition coefficients found in the literature (e.g. Allègre et al., 1995; Corgne et al., 2008).

3.3. Average core and mantle compositions

The final compositions are shown in Fig. 2 as a function of the mantle Fe content, and in Table 4. Results are close to the composition of Abee (EH4), the largest enstatite chondrite (107 kg) fallen on Earth. Compared to the pyrolitic compositions given in Table 5, the E-Earth bulk mantle (BSE) compositions are very enriched in Si and Fe relative to Mg, and depleted in Al and Ca relative to Mg: the ratios Si/Mg ($\approx$1.2), Fe/Mg ($\approx$0.4) and Mg/(Al + Ca) ($\approx$7.0) are significantly larger than typical pyrolitic values (Si/Mg $\approx$ 1.0, Fe/Mg $\approx$ 0.3, and Mg/(Al + Ca) $\approx$ 6.0). The oxygen fugacity corresponding to the model compositions have been raised from IW-4.3 ($Fe_{silicate}$ = 0.83%) to IW-2.4 ($Fe_{silicate}$ = 8.63%) for $\gamma_{FeO} = \gamma_{Fe} = 1$. The corresponding ΔIWs would be −3.2 and −1.3 if we had taken $\gamma_{FeO} = 3$ and $\gamma_{Fe} = 0.8$ as proposed by Corgne et al. (2008).

3.4. Average P–T conditions of core formation

Average P–T conditions of core formation can be obtained from our Si_{core} and Fe_{mantle} model concentrations by using the exchange molar exchange coefficient K_D of Reaction (9). Coefficient K_D has been experimentally determined as a function of P and T by Frost et al. (2008). One way to decouple P and T is to use the distribution constant for the oxygen dissolution equation $K_O(P,T) = x_{Fe_{metal}} x_{O_{metal}}/x_{FeO}$, which is not much sensitive to pressure. To date this constant has only been measured between liquid metal and ferropericlase. The results of Asahara et al. (2007) and Ozawa et al. (2008) allow us to infer a temperature of 3300 ± 300 K, hence from Frost et al. (2008) K_D, a pressure range of 10 to 40 GPa. This takes us back to the debate of shallow versus deep magma ocean, as reviewed for example by Righter (2003).

Additional minor elements, Ni, Co and Cr, are used to further constrain the P, T conditions, based on the recent parameterization of partition coefficients of Corgne et al. (2009), and the oxygen fugacity determined in our model. We obtain a similar temperature range of $\approx$3300 ± 300 K, and we restrict the average equilibration pressure to $\approx$36 ± 4 GPa, for D_{Ni} = 27–28, D_{Co} = 22–25 and D_{Cr} = 2–4. That determination relies heavily on the strong pressure dependence of these partition coefficients. However, the parameterizations $D = f(P,T)$ rely on the assumption that the activity coefficients in the liquid metal phase do not depend strongly on pressure (Corgne et al., 2008, 2009), which at present appears as a wishful thinking at best.

3.5. Lower mantle composition

If one accepts a pyrolitic composition for the Primitive Upper Mantle (PUM), down to a depth yet to be determined, one has to consider that the Primitive Lower Mantle (PLoM) was very different from pyrolite (except for RLE ratios): it was richer in Si, poorer in Ca and Mg, and all the more so that the pyrolitic PUM fraction is large. We define a "perovskite index" to quantify the difference between PUM and PLoM, Pv = (Si + 0.5Al)/(0.5Al + sum of all other cations). Pv is $\approx$0.67 for the pyrolite and $\approx$0.86 for the average E-Earth (Pv = 1 for pure perovskite.) The Pv value for PLoM will be even larger and imply a different phase assemblage than in a pyrolitic lower mantle: a smaller amount of Ca–perovskite, a smaller amount of ferropericlase and a silicate perovskite richer in iron. The extent of the PUM may vary between 25% (the present mass fraction of the upper mantle) and 50% (based for example on the Argon budget). If the PUM represents more than 36% of the mantle (i.e. depths ≥ 1000 km), the PLoM's perovkite index would be larger than 1, and stishovite would be present in the lower mantle.

At this stage, the E-Earth modeling *stricto sensu* is completed: we have established a continuum of compositions for E-objects from which we have extracted a tighter range of compositions compatible with the size of the core and its possible range of light elements' content linked to the mantle Fe content by the exchange Reaction (4). That range can be refined further with geophysical constraints.

4. Geophysical constraints

4.1. Light elements in the core: experimental results and ab initio calculations

Ab initio calculations of Alfè et al. (2002) lead to the conclusion that the core contains 2.5 ± 1.0% of O and 5.6 ± 1.6% of (Si + S) by weight.

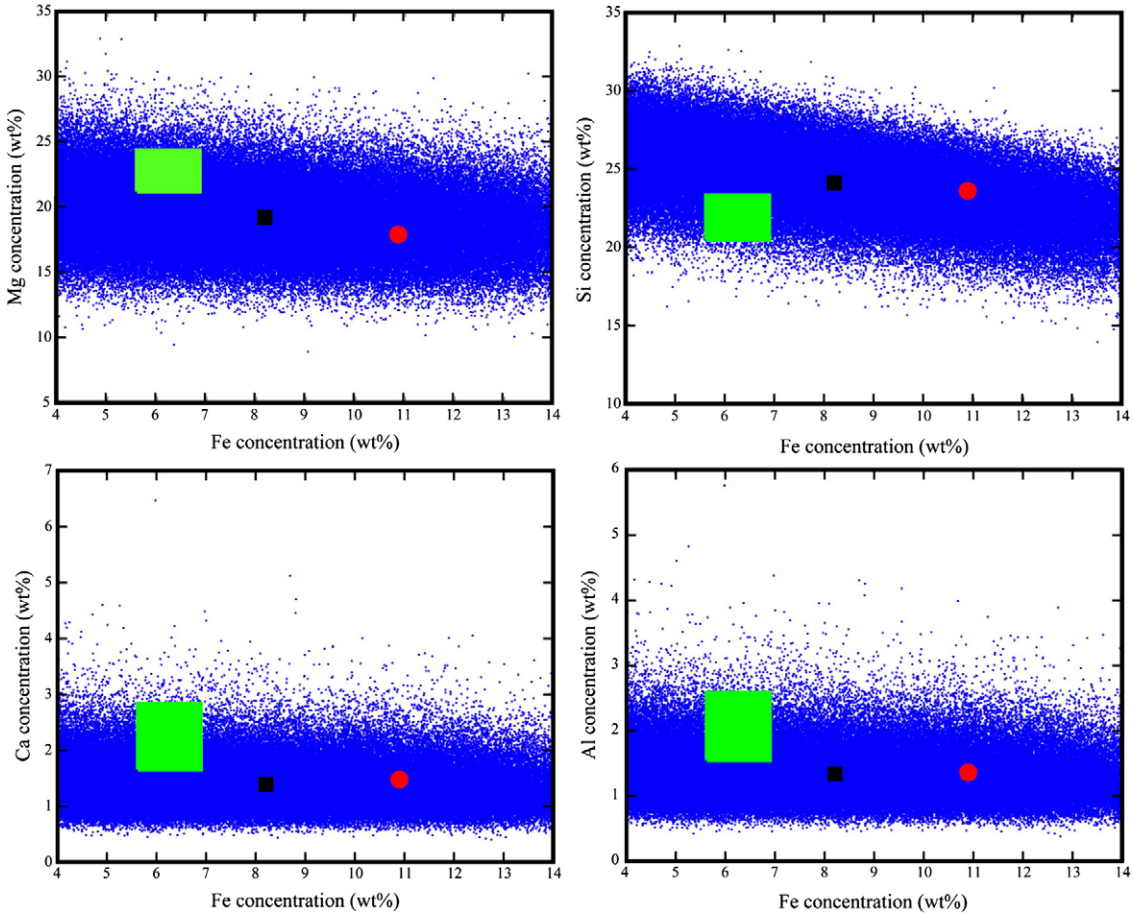

Fig. 2. Range of compositions for the Bulk Silicate Earth from E-chondrites (small dots) as a function of Fe content in the mantle. The plain circle corresponds to the estimate of Javoy (1999) from an average EH composition, the big box shows the range of compositions found in the literature for the pyrolitic upper mantle, and the black square is the average composition for the present model.

However, the Fe–FeS phase diagram at high pressure shows that S is not likely to account for the density jump at the Inner Core Boundary (Morard et al., 2008). Furthermore, the presence of S can explain neither the density and velocity profile of the Earth's inner core (Badro et al., 2007), nor that of the outer core (Sanloup et al., 2004). Based on these results, we thus consider that the core contains no S, and hence 5.6 ± 1.6 wt.% of Si, a result in line with the recent independent experimental geochemical study of Shahar et al. (2009).

4.2. Bulk mantle composition: seismological and geodynamical constraints

Because of the large uncertainties that remain on lower mantle shear moduli, mantle compositions derived from PREM inversion remain controversial. Matas et al. (2007) have proposed a range of molar compositions for the lower mantle that is compatible with most of the other inversion studies: FeO = 0.055–0.070, MgO = 0.426–0.480, and SiO_2 = 0.399–0.461. We use these results to constrain further our model composition. We first infer the composition of a Primitive Lower Mantle (PLoM) by substracting from our BSE compositions a random proportion between 25 and 50% of a pyrolitic PUM as given in Lyubetskaya and Korenaga (2007). Among the PLoM compositions compatible with Matas et al. (2007), we then select those that yield a PLoM denser than PUM. This is necessary for the following reason: the average lower mantle T gradient inferred from PREM is super-isentropic (e.g. Shankland and Brown, 1985; Matas et al., 2007). In a homogeneous convective system with internal heating, viscous dissipation and secular cooling, however, the average temperature profile is sub-isentropic (e.g. Parmentier and Sotin, 2000; Jaupart et al., 2007). On the other hand the PREM super-isentropic temperature profile is consistent with thermo-chemical convection, i.e. a chemically denser lower mantle (e.g. Davaille, 1999).

The compositions resulting from the geophysical filters are shown in Fig. 3. In order to obtain a more precise composition, we further reduce this range of compositions using the present knowledge of the chemical composition of natural enstatite chondrites (Weeks and Sears, 1985; Kallemeyn and Wasson, 1986; Patzer et al., 2001): we have mixed in random proportions the natural chondrites and retained only the mixtures that fall within the range of the previous geophysical filter. The intersection between the natural compositions and the model composition provides a most probable composition with an associated standard deviation given in Table 6. We now discuss the implications of this final result.

Table 4
Composition (in wt.%) of Bulk Silicate Earth (BSE) and of the Earth core obtained from synthetic E-chondrites, for an equilibration pressure of 36 ± 4 GPa and an average temperature of 3300 ± 300 K. The Bulk Earth composition is close to the composition of Abee meteorite (Weeks and Sears, 1985).

Element	Bulk Silicate Earth	Core	Bulk Earth	Abee
Mg	19.1 ± 2.61	–	13.0	12.5
Al	1.28 ± 0.39	–	0.86	0.77
Si	24.1 ± 2.25	7.92 ± 1.57	18.9	19.2
Ca	1.28 ± 0.41	–	0.86	0.81
Fe	8.63 ± 2.70	83.2 ± 2.43	32.8	33.0
Ni	0.19 ± 0.05	5.34 ± 0.32	1.86	1.80
O	44.6 ± 1.12	2.55 ± 1.39	31.0	31.3
Ti	0.07 ± 0.02	–	0.05	0.05
Cr	0.27 ± 0.14	0.55 ± 0.10	0.36	0.34
Co	0.011 ± 0.005	0.25 ± 0.02	0.09	0.08

Table 5
Comparison of BSE compositions between different models.

Mg	Si	Al	Ca	Fe	Ni	Reference
22.8	21.5	2.16	2.31	5.82	0.20	Allègre et al. (1995)
23.4 ± 0.93	21.1 ± 0.58	1.87 ± 0.32	2 ± 0.34	6.22 ± 0.42	0.20 ± 0.02	Lyubetskaya and Korenaga (2007)
22.8 ± 0.6	21.5 ± 0.6	2.15 ± 0.02	2.29 ± 0.02	5.86	0.22	Hart and Zindler (1986)
23.1	21.1	2.1	2.5	6.08	0.21	Jagoutz et al. (1979)
22.8 ± 2.23	21 ± 2.10	2.35 ± 0.24	2.53 ± 0.25	6.26 ± 0.63	0.20 ± 0.02	McDonough and Sun (1995)
21.2	23.3	1.93	2.07	6.22	0.20	Taylor and McLennan (1985)
22.2 ± 0.27	21.2 ± 0.14	2.38 ± 0.20	2.61 ± 0.22	6.30 ± 0.04	0.19 ± 0.01	Palme and O'Neill (2003)
23.0	21.1	1.75	2.21	6.22	–	Ringwood (1975)
22.2	21.3	2.17	2.50	5.83	–	Wanke et al. (1984)
17.9	23.6	1.36	1.48	10.9	0.27	Javoy (1999)

5. Discussion and perspectives: composition and dynamics of the Earth

5.1. The heterogeneous mantle

Matas et al. (2007) have shown that a homogeneous pyrolitic composition is too rich in MgO and too poor in SiO_2 to fit the PREM data, a result confirmed experimentally by Ricolleau et al. (2009). However, various compositions can fit the PREM equally well, especially if one takes into account anelastic contributions (Matas and Bukowinski, 2007). The additional constraints brought by the E-chondrite model can be used to choose between these different solutions. For example, Khan et al. (2008) and Verhoeven et al. (2009) propose a lower mantle depleted in SiO_2, which is not consistent with the E-Earth model. In the same way, from the two sets of compositions proposed by Matas et al. (2007), only that with a Mg/Si ratio decreasing in the lower mantle is compatible with our results.

Another way to further our knowledge of the chemical and thermal structure of the mantle is to compare the predictions of mantle flow models with the characteristics of 3D tomographic images. Up to now, models of purely thermal convection (Schuberth et al., 2009) and models of thermo-chemical convection with a denser lower mantle (Deschamps et al., 2007; Steinberger and Holme, 2008) are able to account for seismic anomalies equally well. Many pitfalls and uncertainties involved in flow models and tomographic inversions prevent a definitive answer (Simmons et al., 2009), but it seems that a chemically heterogeneous lower mantle is more consistent with tomographic models (Hernlund and Houser, 2007).

5.2. RLE enrichment factor and volatility of elements during Earth formation

The enrichment of Bulk Silicate Earth in RLE elements (Ca, Al, Ti, Rare Earth Elements (REE), U, Th, etc.) relative to CI chondrites is classically quantified using the enrichment factor defined as $E.F. = (C_{RLE})_{mantle}/(C_{RLE})_{CI}$ (e.g. Hart and Zindler, 1986; McDonough and Sun, 1995; Lyubetskaya and Korenaga, 2007). Its value for different models varies from 2.1 to 2.8 (see Lyubetskaya and Korenaga (2007) for a

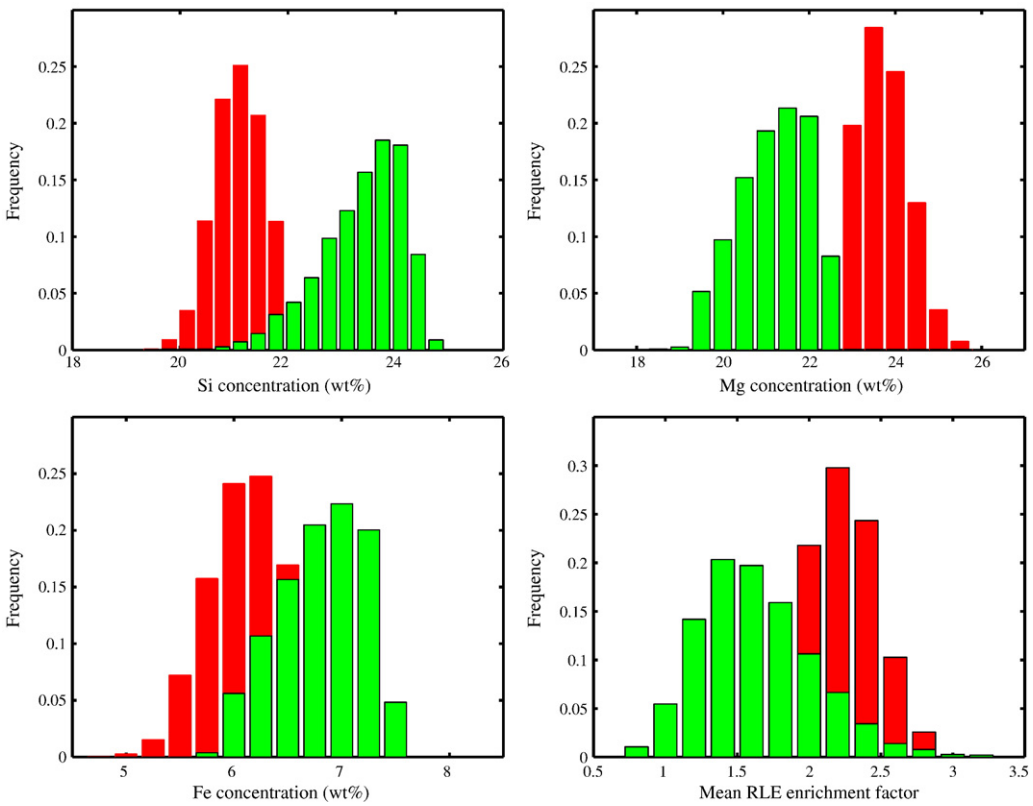

Fig. 3. Distribution of compositions (Si, Mg, and Fe) for a pyrolitic uppermantle (PUM, back red histogram) according to Lyubetskaya and Korenaga (2007), and for an EH lowermantle (PLoM, front green histogram). The RLE enrichment factor is calculated for the whole mantle.

Table 6
Most probable composition (in wt.%) of Primitive Upper Mantle (PUM), Primitive Lower Mantle (PLoM) and core, for an E-Earth compatible with geophysical and geodynamical constraints, and with the present day sampling of E-chondrites. The Primitive Upper Mantle represents 32.5 ± 6.33% of the Bulk Silicate Earth.

Element	PUM	PLoM	Core
Mg	23.5 ± 0.65	21.3 ± 0.67	–
Al	1.90 ± 0.32	0.98 ± 0.39	–
Si	21.4 ± 0.49	24.2 ± 0.48	6.64 ± 0.51
Ca	1.95 ± 0.32	1.04 ± 0.39	–
Fe	6.17 ± 0.38	7.21 ± 0.39	85.5 ± 1.14
Ni	0.20 ± 0.02	0.19 ± 0.13	5.35 ± 0.81
O	44.4 ± 0.19	45.0 ± 0.20	1.99 ± 0.46
Ti	0.10 ± 0.02	0.06 ± 0.02	–
Cr	0.27 ± 0.04	0.27 ± 0.05	0.55 ± 0.05
Co	0.01 ± 0.001	0.01 ± 0.005	0.25 ± 0.03

review). Part of that "enrichment" is due to the concentration of RLE in the silicate part by core formation, i.e., as the core represents 67.6% of the mass of the Earth, a factor of 100/67.6 = 1.479 (e.g. McDonough and Sun, 1995). In order to explain the extra enrichment Hart and Zindler (1986), like Ringwood (1979), propose that the Earth is "equivalent to devolatilized CI chondrite material" either by volatilization or non condensation. This amounts to 41.8% volatiles removed and yields a total enrichment factor of $100/67.6 \times 100/(100-41.8) = 2.55$. The conditions are different for our E-material as it is virtually volatile-free. As average EH chondrites have RLE concentrations essentially equal to those in CI (Wasson and Kallemeyn, 1988), our enrichment factor relative to CI is the same as relative to EH and reduces essentially to that due to core formation, i.e. ≈1.5.

The RLE enrichment factor can be used to infer the behavior of supposedly less refractory elements, such as Si, Mg, Fe and Mn. For example, combining the mantle composition of Lyubetskaya and Korenaga (2007) with a reasonable Si content in the core (say 7%), we find that Mg/Al and Si/Al ratios are larger in the Bulk Earth than in the CI chondrites, which would imply that—if CI were indeed the Earth building material—Mg would be more enriched than RLE (2.4 instead of 2.1). In our opinion this is a good indication that (1) EH material is more consistent with the PUM composition of Lyubetskaya and Korenaga (2007) than CI material, and (2) that Mg and Si elements were not labile during accretion. Things are different for Mn as the E-Earth model predicts a large enrichment in Mn in the lower mantle, which seems difficult to justify. As Mn is the less refractory of the four elements considered above, we conclude that the temperature and rate of accretion were such that Mn was partially lost. Such a result can later be used as a constraint for the modeling of planetary accretion.

5.3. Heat production in the lower mantle

The low RLE enrichment factor predicted by E-Earth model has two important consequences: (1) depletion in Ca and Al in the lower mantle, which implies a low concentration of Al in Mg–silicate perovskite and depletion of Ca–silicate perovskite (if not absence), and (2) strong depletion in radioactive elements U and Th (and K for a given K/U ratio) with respect to conventional primitive mantle models. An E-Earth lower mantle is thus characterized by less internal heating, which may affect its secular cooling as well as the cooling of the core. Labrosse and Jaupart (2007) showed that the current imbalance of the surface heat flow and radiogenic heating can be explained by a maximum age of subduction independent of thermal buoyancy. Within this framework, E-Earth models can easily fit the thermal constraints. The partitioning of cooling between core and mantle remains an open question. All else being equal, low internal heat generation in the lower mantle implies a large heat flow from the core. This is in line with the observation of double seismic discontinuities in D'', explained by a double crossing of the perovskite–postperovskite phase transition provided that the temperature gradient at the CMB is larger than the Clapeyron slope (Hernlund et al., 2005). This argument predicts large values of the heat flow at the CMB, in agreement with the most recent (and largest) estimates in the 7–15 TW range (Lay et al., 2008).

5.4. Origin of mantle chemical heterogeneity

Many processes have been advocated for the generation of a heterogeneous early mantle (e.g. Javoy, 1995; Anderson, 2002). A complete discussion of this issue is out of the scope of this paper, and we only discuss here the possibility of heterogeneous accretion, as it is easily feasible in the chemically diverse world of E-chondrites.

Our final E-Earth composition corresponds roughly to a mixture of ≈2/3 of EH chondrites and ≈1/3 of EL chondrites. As EH chondrites are richer in iron, hence denser than EL chondrites, a mixture of EH and EL will tend to gravitationally segregate during the first stage of the planetary differentiation, yielding a chemically stratified proto-Earth with a lower mantle enriched in (denser) EH-type material and an upper mantle enriched in EL-type material. EL chondrites are more in line with a pyrolitic mantle through their larger Mg, Ca and Al content, but they are somewhat too rich in Si. However, the dissolution of Si in metal through Reaction (4) is enhanced at intermediate pressure, with a peak at 25 GPa (Javoy, 1995), and this may provide the required reduction of Si content in the upper mantle. The resulting primordial heterogeneities between the upper and the lower mantle have been affected by partial convective mixing, which resulted in the thermo-chemical domes present today in the lower mantle as the remnants of the Primitive Lower Mantle (PLoM) (e.g. Davaille, 1999; Samuel et al., 2005; Deschamps et al., 2007).

Within the framework of "gravitational" differentiation of the mantle, the material keeps its chondritic characteristics at all depths, and especially its RLE ratios (Ca/Al and Al/Ti). This particular feature is in line with the hypotheses used to infer the PUM composition in classical models (e.g. Lyubetskaya and Korenaga, 2007). Thus, all the consequences linked to their use of chondritic elemental ratios are preserved.

5.5. The way to future experimental tests of E-Earth model

Most experimental results on the problem of core formation have been obtained with compositions which do not correspond to the Earth's oxygen content, and existing Si solubility experiments generally ignore the role of the initial balance of oxidation of the Si–Fe system. It is also in that sense that the E-chondrites are, Redoxwise, identical to Earth. This is why it is essential to use their composition to experimentally study the formation of the core.

More generally the "extent of oxidation" of the bulk experimental starting material should be equivalent to that displayed by existing Bulk Earth models to properly test the possibility induced by Reaction (4), that purely internal processes can lead to an increase of the oxidation state of the mantle without any need for the external input of more oxidized material. To Bulk Earth scale, oxygen exchange is limited to that linked to Si and Fe, i.e. about 2/3 of the Earth's total oxygen. A practical way to express the extent of oxidation of the terrestrial Si–Fe system is the atomic ratio of that exchangeable oxygen to that of total Fe + Si, defined as

$$\mathrm{EXOR} = \frac{2n\mathrm{SiO_2} + n\mathrm{FeO}}{n\mathrm{Si} + n\mathrm{Fe}}, \tag{11}$$

where $n\mathrm{SiO_2}$, nFeO, nSi, and nFe are the mole fractions of SiO_2, FeO, total Si and total Fe respectively. For all Bulk Earth models otherwise different but with sizeable amounts of Si in the core (Ringwood, 1975; Allègre et al., 1995; Javoy, 1995) EXOR variations are restricted to 1.03 ± 0.03. Among chondrites only enstatite chondrites can display a similar EXOR. However, most experimental starting materials are unfit and present

either too low or too large EXOR. For example, the recent study of Corgne et al. (2008) used two starting materials: SM1, supposedly similar to a CI type material reduced to an "Earthly" level, and SM2 figurating an E-chondrite type. The EXOR of SM1 is 1.17, much too high for Earth to allow Si dissolution in Fe metal without undue levels of $Fe_{silicate}$, whereas the EXOR of SM2 is 0.89 and corresponds to a too reduced material with a much too large initial Si_{metal}.

6. Conclusion

Isotopes identify E-chondrites and Earth as members of the same group of Solar System material: they impose that Bulk Earth composition be taken in the compositional range of E-chondrites. Isotopes emphasize a crucial chemical feature of the Earth, its extent of oxidation: no chondritic contraption of isotopic coincidence will ever possess the Earth's EXOR ratio. Even in the E-chondrite space, only objects belonging to the Fe-rich end of the family have this property. This property is a pre-requisite for the core differentiation mechanism, accounts for the core–mantle relationship and finally explains why f_{O_2} increases during core formation, which is being advocated more and more often but never explained.

The resulting Bulk Earth and BSE compositions can be narrowed down according to terrestrial constraints, and thus depend on the accuracy of these constraints. The simplest and best established constraints are that the core represents exactly 32.4% of the total mass and bears $10 \pm 4\%$ light elements. A more stringent constraint, which must be confirmed, is that the core contains in fact $6 \pm 2\%$ Si and a total of $8 \pm 2\%$ of light elements, excluding S. Lastly, the mineralogical composition and thermal profiles resulting from the inversion of PREM must be accounted for.

In all cases, at variance with a pyrolitic homogeneous whole mantle, the E-Earth mantle below 650 km certainly contains more silicate perovskite, less Al, less Ca–silicate perovskite (possibly none), and even, perhaps, stishovite. It will also contain more Fe, and long period radioactive elements in smaller amounts. All these features bear important consequences on mantle dynamics, mantle outgassing and Earth energy budget. E-Earth models provide a testable framework for various investigations on Earth dynamics. In particular, the geodynamical consequences of a lower mantle which is both more viscous (richer in Si) and denser (richer in Fe), but also depleted in radioactive elements, await scrutiny.

Acknowledgements

We thank Lars Stixrude for his editorial handling, H. Palme and two anonymous reviewers for their comments. This article benefitted from fruitful discussions with Jan Matas. This work is IPGP contribution 2617.

References

Alfè, D., Gillan, M.J., Price, G.D., 2002. Composition and temperature of the Earth's core constrained by combining ab initio calculations and seismic data. Earth Planet. Sci. Lett. 195, 91–98.
Allègre, C.J., Poirier, J.P., Humler, E., Hofmann, A.W., 1995. The chemical composition of the Earth. Earth Planet. Sci. Lett. 134, 515–526.
Anderson, D.L., 2002. The case for irreversible chemical stratification of the mantle. Int. Geol. Rev. 44, 97–116.
Asahara, Y., Frost, D., Rubie, D., 2007. Partitioning of FeO between magnesiowüstite and liquid iron at high pressures and temperatures: implications for the composition of the Earth's outer core. Earth Planet. Sci. Lett. 257, 435–449. doi:10.1016/j.epsl.2009.09.029.
Badro, J., Fiquet, G., Guyot, F., Gregoryantz, E., Occelli, F., Antonangeli, D., D'Astuto, M., 2007. Effect of light elements on the sound velocities in solid iron: implications for the composition of the Earth's core. Earth Planet. Sci. Let. 254, 233–238.
Birck, J., Rotaru, M., Allègre, C., 1999. ^{53}Mn–^{53}Cr evolution of the solar system. Geochim. Cosmochim. Acta 63, 4111–4117.
Cammarano, F., Romanowicz, B., 2007. Insights into the nature of the transition zone from physically constrained inversion of long-period seismic data. PNAS 104 (22), 9139–9144. doi:10.1073/pnas.0608075104.
Cartigny, P., Boyd, S.R., Harris, J., Javoy, M., 1997. Nitrogen isotopes in peridotitic diamonds from China: the mantle signature. Terra Nova 94, 175–179.
Clayton, R., Mayeda, T., 1984. Oxygen isotope composition of enstatite chondrites and aubrites. J. Geophys. Res. 89, C245–C249.
Corgne, A., Keshav, S., Wood, B., McDonough, W., Fei, Y., 2008. Metal-silicate partitioning and constraints on core composition and oxygen fugacity during Earth accretion. Geochim. Cosmochim. Acta 72, 574–589.
Corgne, A., Siebert, J., Badro, J., 2009. Oxygen as a light element: a solution to single-stage core formation. Earth Planet. Sci. Lett. 288 (1–2), 108–114. doi:10.1016/j.epsl.2009.09.012.
Crabb, J., Anders, E., 1981. Noble gases in E-chondrites. Geochim. Cosmochim. Acta 45, 2443–2464.
Dauphas, N., Davis, A.M., Marty, B., Reisberg, L., 2004. The cosmic molybdenum–ruthenium isotope correlation. Earth Planet. Sci. Lett. 226, 465–475.
Davaille, A., 1999. Simultaneous generation of hotspots and superswells by convection in a heterogeneous planetary mantle. Nature 402, 756–760.
Deschamps, F., Trampert, J., 2004. Towards a lower mantle reference temperature and composition. Earth Planet. Sci. Lett. 222, 161–175.
Deschamps, F., Trampert, J., Tackley, P., 2007. Thermo-chemical structure of the lower mantle: seismological evidences and consequences for geodynamics. In: Yuen, D.A., et al. (Ed.), Superplumes: Beyond Plate Tectonics. Springer, pp. 293–320.
Dreibus, G., Palme, 1996. Cosmochemical constraints on the sulfur content in the Earth's core. Geochim. Cosmochim. Acta 60 (7), 1125–1130.
Easton, A.J., 1985. E-chondrites: significance of the partition of the elements between "silicate" and "sulfide". Meteoritics 20, 89–100.
Fogel, R., Hess, P., Rutherford, M., 1989. Intensive parameters in enstatite chondrite metamorphism. Geochim. Cosmochim. Acta 53, 2735–2746.
Frost, D.J., Mann, U., Asahara, Y., Rubie, D.C., 2008. The redox state of the mantle during and just after core formation. Phil. Trans. R. Soc. A 366, 4315–4337. doi:10.1098/rsta.2008.0147.
Gessmann, C., Wood, B., Rubie, D., Kilburn, M., 2001. Solubility of silicon in liquid metal at high pressure: implications for the composition of the Earth's core. Earth Planet. Sci. Lett. 184, 367–376.
Hart, S.R., Zindler, A., 1986. In search of a bulk-Earth composition. Chem. Geol. 57, 247–267.
Hernlund, J.W., Houser, C., 2007. On the statistical distribution of seismic velocities in Earth's deep mantle. Earth Planet. Sci. Lett. 265, 423–437. doi:10.1016/j.epsl.2007.10.042.
Hernlund, J.W., Thomas, C., Tackley, P.J., 2005. Phase boundary double crossing and the structure of Earth's deep mantle. Nature 434, 882–886. doi:10.1038/nature03472.
Jagoutz, E., Palme, H., Baddenhausen, H., Blum, K., Cendales, M., Dreibus, G., Spettel, B., Lorenz, V., Wänke, H., 1979. The abundances of major, minor and trace elements in the Earth's mantle as derived from primitive ultramafic nodules. Proc. Lunar Planet. Sci. Conf. 10, 2031–2050.
Jaupart, C., Labrosse, S., Mareschal, J.-C., 2007. Temperatures, heat and energy in the mantle of the Earth. In: Schubert, G. (Ed.), Treatise on Geophysics, Vol. 7. Elsevier Ltd., pp. 253–304.
Javoy, M., 1995. The integral enstatite chondrite model of the Earth. Geophys. Res. Lett. 22, 2219–2222.
Javoy, M., 1999. Chemical Earth models. C.R. Acad. Sci. 329, 537–555.
Javoy, M., 2005. Where do the oceans come from? C.R. Acad. Sci. 337, 139–158.
Javoy, M., Pineau, F., 1983. Stable isotope constraints on a model Earth, from the study of mantle nitrogen. Meteoritics 18, 320–321.
Javoy, M., Pineau, F., 1991. The volatiles record of a "popping" rock from the mid Atlantic ridge at 14°N: chemical and isotopic composition of gas trapped in the vesicles. Earth Planet. Sci. Lett. 107, 598–611.
Javoy, M., Pineau, F., Demaiffe, G., 1984. Nitrogen and carbon isotopic composition in the diamonds of Mbuji Mayi (Zaïre). Earth Planet. Sci. Lett. 68, 399–412.
Javoy, M., Pineau, F., Delorme, H., 1986. Carbon and nitrogen isotopes in the mantle. Chem. Geol. 57, 41–62.
Kallemeyn, G., Wasson, J., 1986. Compositions of enstatite (EH3, EH4, 5 and EL6) chondrites: implications regarding their formation. Geochim. Cosmochim. Acta 50, 2153–2164.
Keil, K., 1968. Mineralogical and chemical relationships among enstatite chondrites. J. Geophys. Res. 73 (22), 6945–6976.
Khan, A., Connolly, J.A.D., Taylor, S.R., 2008. Inversion of seismic and geodetic data for the major element chemistry and temperature of the Earth's mantle. J. Geophys. Res. 113, B09308.
Kong, P., Mori, T., Ebihara, M., 1997. Compositional continuity of enstatite chondrites and implications for heterogeneous accretion of the enstatite chondrite parent body. Geochim. Cosmochim. Acta 61, 4895–4914.
Labrosse, S., Jaupart, C., 2007. Thermal evolution of the Earth: secular changes and fluctuations of plate characteristics. Earth Planet. Sci. Lett. 260, 465–481.
Lay, T., Hernlund, J., Buffet, B., 2008. Core–mantle boundary heat flow. Nat. Geosci. 1, 25–32.
Lin, Y., Kimura, M., 1998. Petrographic and mineralogical study of new EH melt rocks and a new enstatite chondrite grouplet. Meteorit. Planet. Sci. 33, 501–511.
Lodders, K., 2003. Solar system abundances and condensation temperatures of the elements. Astrophys. J. 591, 1220–1247.
Lodders, K., Fegley, B., 1993. Lanthanide and actinide chemistry at high C/O ratios in the solar nebula. Earth Planet. Sci. Lett. 117, 125–145. doi:10.1016/j.epsl.2009.09.029.
Lyubetskaya, T., Korenaga, J., 2007. Chemical composition of the Earth primitive mantle and its variance: 1. Method and results. J. Geophys. Res. 112. doi:10.1029/2005JB004223, B03211.
Malavergne, V., Siebert, J., Guyot, F., Gautron, L., Combes, R., Hammouda, T., Borensztajn, S., Frost, D., Martinez, I., 2004. Si in the core? New high-pressure and high-temperature experimental data. Geochim. Cosmochim. Acta 68, 4201–4211.
Mason, B., 1966. The enstatite chondrites. Geochim. Cosmochim. Acta 30, 23–39.
Matas, J., Bukowinski, M.S.T., 2007. On the anaelastic contribution to the temperature dependence of lower mantle seismic velocities. Earth Planet. Sci. Lett. 259, 51–65. doi:10.1016/j.epsl.2007.04.028.

Matas, J., Bass, J., Ricard, Y., Mattern, E., Bukowinski, M.S.T., 2007. On the bulk composition of the lower mantle: predictions and limitations from generalized inversion of radial seismic profiles. Geophys. J. Int. 170 (17), 764–780.
McDonough, W.F., Sun, S., 1995. The composition of the Earth. Chem. Geol. 120, 223–253.
Meisel, R., Walker, R., Morgan, J., 1996. The osmium isotopic composition of the Earth's primitive upper mantle. Nature 383, 517–520.
Morard, G., Andrault, D., Guignot, N., Sanloup, C., Mezouar, M., Petitgirard, S., Fiquet, G., 2008. In situ determination of Fe–Fe_3S phase diagram and liquid structural properties up to 65 GPa. Earth Planet. Sci. Lett. 272, 620–626.
Moreira, M., Allègre, C.J., 1998. Helium–neon systematics and the structure of the mantle. Chem. Geol. 147, 53–59.
O'Brien, D.P., Morbidelli, A., Levison, H.F., 2006. Terrestrial planet formation with strong dynamical friction. Icarus 184, 39–58.
Ozawa, H., Hirose, K., Mitome, M., Bando, Y., Sata, N., Ohishi, Y., 2008. Chemical equilibrium between ferropericlase and molten iron to 134 GPa and implications for iron content at the bottom of the mantle. Geophys. Res. Lett. 35, L05308. doi:10.1029/2007GL032648.
Palme, H., O'Neill, H.S.C., 2003. Cosmochemical estimates of mantle composition. Treatise on Geochemistry, Vol. 2. Elsevier, New-York, pp. 1–38.
Park, J., Okazaki, R., Nagao, K., Baroschewitz, R., 2005. Noble gas study of new Enstatite SaU290 with high solar gases. Lunar Planet. Sci. XXXVI, 1632.
Parmentier, E.M., Sotin, C., 2000. Three-dimensional numerical experiments on thermal convection in a very viscous fluid: implications for the dynamics of a thermal boundary layer at high Rayleigh number. Phys. Fluids 12, 609–617.
Patzer, A., Schultz, L., 2002. Noble gases in enstatite chondrites II: The trapped component. Meteorit. Planet. Sci. 37, 601–612.
Patzer, A., Hill, D.H., Boyton, W.V., 2001. Itqiy: a metal-rich enstatite meteorite with achondritic texture. Meteorit. Planet. Sci. 36, 1495–1505.
Petyaev, M., Khodakovsky, I., 1986. Thermodynamic properties and conditions of formation of minerals in enstatite meteorites. Chemistry and Physics of the Terrestrial Planets. : Advances in Physical Chemistry, 6. Springer Verlag, pp. 107–135.
Poirier, J.P., 1994. Light elements in the Earth's outer core: a critical review. Phys. Earth Planet. Inter. 85, 319–337.
Raquin, A., Moreira, M., 2009. Atmospheric $^{38}Ar/^{36}Ar$ in the mantle: implications for the nature of the terrestrial parent bodies. Earth Planet. Sci. Lett. 287 (3–4), 551–558. doi:10.1016/j.epsl.2009.09.003.
Ricolleau, A., Fei, Y., Cottrell, E., Watson, H., Deng, L., Zhang, L., Fiquet, G., Auzende, A., Roskosz, M., Morard, G., Prakapenka, V., 2009. Density profile of pyrolite under the lower mantle conditions. Geophys. Res. Lett. 36, L06302. doi:10.1029/2008GL036759.
Righter, K., 2003. Metal–silicate partitioning of siderophile elements and core formation in the early Earth. Annu. Rev. Earth Planet. Sci. 31, 135–174.
Ringwood, A., 1975. Pyrolite and the chondritic Earth model. Composition and Petrology of the Earth's Mantle. : International Series in the Earth's and Planetary Sciences. McGraw Hill, pp. 189–194.
Ringwood, A.E., 1979. Origin of the Earth and Moon. Springer, New York.
Robie, R., Hemingway, B.S., 1995. Thermodynamic properties of minerals and related substances at 298.1°K and 1 bar (10^5 Pascals) pressure and at higher temperatures. USGS Bull. 2131 461 pp.
Rubin, A.E., 1983. The Adhi Kot breccia and implications for the origin of chondrules and silica-rich clasts in enstatite chondrites. Earth Planet. Sci. Lett. 64, 131–201.
Rubin, A.E., Keil, K., 1983. Mineralogy and petrology of the Abee enstatite chondrite breccia. Earth Planet. Sci. Lett. 62, 118–131.
Sakao, H., Elliott, J.F., 1975. Thermodynamics of dilute BCC Fe–Si alloys. Metall. Mater. Trans. B 6, 1849–1851.
Samuel, H., Farnetani, C.G., Andrault, D., 2005. Heterogeneous lowermost mantle: compositional constraints and seismological observables. Geophysical Monograph, Vol. 160. American Geophysical Union, Washington, DC, USA, pp. 101–116.
Sanloup, C., Fiquet, G., Gregoryanz, E., Morard, G., Mezouar, M., 2004. Effect of Si on liquid Fe compressibility: implications for sound velocity in core materials. Geophys. Res. Lett. 31, L07604.
Schuberth, B.S.A., Bunge, H.-P., Ritsema, J., 2009. Tomographic filtering of high-resolution mantle circulation models: can seismic heterogeneity be explained by temperature alone? Geochem. Geophys. Geosyst. 10, Q05W03.
Schwerdtfeger, V.K., Engell, H.-J., 1964. Die freie Bildungsenthalpie von Siliziumdioxyd und die Aktivitaten von Silizium in flüssigen und Kobalt. Arch. Eisenhüttenwes. 6, 533–540.
Shahar, A., Ziegler, K., Young, E.D., Ricolleau, A., Schauble, E.A., Fei, Y., 2009. Experimentally determined Si isotope fractionation between silicate and Fe metal and implications for Earth's core formation. Earth Planet. Sci. Lett. 288 (1–2), 228–234. doi:10.1016/j.epsl.2009.09.025.
Shankland, T.J., Brown, J.M., 1985. Homogeneity and temperatures in the lower mantle. Phys. Earth Planet. Inter. 38, 51–58.
Simmons, N.A., Forte, A.M., Grand, S.P., 2009. Joint seismic, geodynamic and mineral physical constraints on three-dimensional mantle heterogeneity: implications for the relative importance of thermal versus compositional heterogeneity. Geophys. J. Int. 177, 1284–1304.
Steinberger, B., Holme, R., 2008. Mantle flow models with core–mantle boundary constraints and chemical heterogeneities in the lowermost mantle. J. Geophys. Res. 113, B054034.
Stixrude, L., Hemley, R.J., Fei, Y., Mao, H.K., 1992. Thermoelasticity of silicate perovskite and magnesowüstite and stratification of the Earth's mantle. Science 257, 1099–1101.
Taylor, S., McLennan, S.M., 1985. The Continental Crust: Its Composition and Evolution. Blackwell, Oxford.
Trieloff, M., Kunz, J., Clague, D., Harrison, D., Allègre, C., 2000. The nature of pristine noble gases in mantle plumes. Science 288, 1036–1038.
Trinquier, A., Birck, J.L., Allègre, C.J., 2007. Widespread ^{54}Cr heterogeneities in the inner solar system. Astrophys. J. 655, 1179–1185.
Trinquier, A., Elliott, T., Ulfbeck, D., Coath, C., Krot, A.N., Bizzarro, M., 2009. Origin of nucleosynthetic isotope heterogeneity in the solar protoplanetary disk. Science 324 (5925), 295–424. doi:10.1126/science.1168221.
Verhoeven, O., Mocquet, A., Vacher, P., Rivoldini, A., Menvielle, M., Arrial, P.-A., Choblet, G., Tarits, P., Dehant, V., Hoolst, T.V., 2009. Constraints on thermal state and composition of the Earth's lower mantle from electromagnetic impedances and seismic data. J. Geophys. Res. 114, B03302.
Wanke, H., Dreibus, G., Jagoutz, E., 1984. Mantle chemistry and accretion history of the Earth. In: Kroner, A. (Ed.), Archean Geochemistry. Springer, Berlin, pp. 1–24.
Wasson, J.T., 1985. Meteorites. Springer, Berlin.
Wasson, J., Kallemeyn, G., 1988. Composition of chondrites. Phil. Trans. R. Soc. London A 325, 535–544.
Weeks, K.S., Sears, D.W., 1985. Chemical and physical studies of type 3 chondrites—V: the enstatite chondrites. Geochim. Cosmochim. Acta 49, 1525–1536.
Wetherill, G.W., Stewart, G.R., 1989. Accumulation of a swarm of small planetesimals. Icarus 77, 190–209.